HHS Public Access

Author manuscript

J Med Chem. Author manuscript; available in PMC 2018 April 04.

Published in final edited form as:

J Med Chem. 2017 October 26; 60(20): 8456–8465. doi:10.1021/acs.jmedchem.7b00847.

Membrane-Active Hydantoin Derivatives as Antibiotic Agents

Ma Su[†,§], **Donglin Xia**[‡,§], **Peng Teng**[†,§], **Alekhya Nimmagadda**[†], **Chao Zhang**[‡], **Timothy Odom**[†], **Annie Cao**[†], **Yong Hu**[*,‡,iD], and **Jianfeng Cai**[*,†,iD]

[†]Department of Chemistry, University of South Florida, 4202 E. Fowler Ave, Tampa, Florida 33620, United States

[‡]Department of Biomedical Engineering, College of Engineering and Applied Science, Nanjing University, 22 Hankou Road, Nanjing, Jiangsu 210093, P. R. China

Abstract

Hydantoin (imidazolidinedione) derivatives such as nitrofurantoin are small molecules that have aroused considerable interest recently due to their low rate of bacterial resistance. However, their moderate antimicrobial activity may hamper their application combating antibiotic resistance in the long run. Herein, we report the design of bacterial membrane-active hydantoin derivatives, from which we identified compounds that show much more potent antimicrobial activity than nitrofurantoin against a panel of clinically relevant Gram-positive and Gram-negative bacterial strains. These compounds are able to act on bacterial membranes, analogous to natural host-defense peptides. Additionally, these hydantoin compounds not only kill bacterial pathogens rapidly but also prevent the development of methicillin-resistant *Staphylococcus aureus* (MRSA) bacterial resistance under the tested conditions. More intriguingly, the lead compound exhibited *in vivo* efficacy that is much superior to vancomycin by eradicating bacteria and suppressing inflammation caused by MRSA-induced pneumonia in a rat model, demonstrating its promising therapeutic potential.

Graphical abstract

[*]**Corresponding Authors**. hvyong@nju.edu.cn (Y.H.). jianfengcai@usf.edu (J.C.).

ORCID

Yong Hu: 0000-0002-5394-6743

Jianfeng Cai: 0000-0003-3106-3306

[§]M.S., D.X., and P.T. contributed equally to this work.

ASSOCIATED CONTENT

Supporting Information

The Supporting Information is available free of charge on the ACS Publications website at DOI: 10.1021/acs.jmedchem.7b00847.

Procedures for *in vitro* studies, the time kill assay, the drug resistance assay, fluorescence microscopy, and *in vivo* studies; ^{1}H and ^{13}C NMR spectra and HPLC traces of compounds 1–25 (PDF)

Molecular formula strings and MIC data (CSV)

The authors declare no competing financial interest.

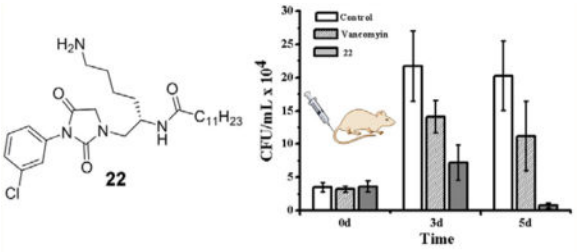

Compound	MIC (μg/mL)					
	Gram Positive			Gram Negative		
	MRSA	MRSE	VREF	*E. Coli*	*P. A.*	*K. P.*
22	0.5	0.5	0.5	1	1	0.78

INTRODUCTION

Infections caused by drug-resistant bacteria have become one of the greatest threats to public health in the 21st century.[1] Exploration of alternative therapeutic strategies is in huge demand. One promising approach is to reinvestigate known antibiotics and design their derivatives, in the hope of identifying novel antibiotic agents that combat antibiotic resistance. The development of hydantoins, the derivatives of 2,4-imidazolidinedione, for antibacterial applications has been taking place for a long time.[2–6] The mechanism of action of hydantoin derivatives is complex and not well understood, possibly due to a combination of various modes including damage to bacterial DNA,[7,8] binding to bacterial ribosomes to inhibit synthesis of critical bacterial enzymes,[9] and so on. To date, one hydantoin derivative, nitrofurantoin, has been approved to treat urinary tract infections.[10–16] As an old antibiotic, it has recently attracted considerable interest due to its low probability of bacterial resistance compared to that of other conventional antibiotics such as fluoroquinolones,[17,18] possibly owing to the mixed mechanisms of action of hydantoins. However, hydantoin derivatives including nitrofurantoin generally exhibit only moderate antibacterial activity, which may limit their further application in combating emergent antibiotic resistance.[19–21] For instance, nitrofurantoin (Figure 1) shows a minimum inhibitory concentration (MIC) of 12.5 μg/mL for methicillin-resistant *Staphylococcus aureus* (MRSA), and it is not active toward *Pseudomonas aeruginosa* up to 100 μg/mL.[19–21]

Another alternative strategy to combat antibiotic resistance is to develop cationic host-defense peptides (HDPs) as potential antibiotic agents. Containing hydrophobic and cationic groups, HDPs[22,23] and related peptidomimetics, such as β-peptides,[24–26] oligoureas,[27] peptoids,[28,29] AApeptides,[30,31] and so forth, are able to selectively interact with negatively charged bacterial membranes, leading to membrane damage and subsequent bacterial cell death. Cationic charges are critical for the association of these molecules with bacterial membranes, whereas hydrophobic groups are of importance for membrane penetration and disruption. HDPs and their derivatives are believed to minimize the probability developing bacterial resistance, as membrane interaction and disruption are rather biophysical and lack specific membrane targets. It should be noted that besides their membrane action, many HDPs can also permeate bacterial membranes and act on intracellular targets.[22,32–34] Indeed, the mixed antibacterial mechanisms of HDPs are expected to further synergize their ability

to overcome bacterial resistance. Despite considerable enthusiasm, HDPs and oligomeric peptidomimetics have encountered obstacles to their practical applications, including moderate activity and systematic toxicity.[35,36] In addition, the high molecular weight (normally >1000 Da) and structural complexity of HDPs have led to tedious synthetic processes and high production costs, hampering their therapeutic development.

Inspired by the structures of hydantoin derivatives such as nitrofurantoin and the mechanism of action of HDPs, we set out to design a new class of hydantoin-based small molecules with membrane activity. It is well-known that the existing lipoantibiotics including marketed drugs daptomycin[37,38] and polymyxin,[39,40] the two "last-resort" antibiotics, all associate and interact with bacterial membranes using their lipid tails. Our previous findings also indicated that cationic peptidomimetics with lipidation could kill bacteria with greater potency by disrupting bacterial membranes.[41–46] Thus, we hypothesized that hydantoin compounds bearing cationic groups and lipid tails (Figure 2, D2) would be membrane active, similar to the mechanism of action of HDPs. As such, they could interact with bacterial membranes and kill bacterial pathogens through bacterial membrane disruption. In addition, as the compounds still contain the hydantoin pharmacophore (Figure 2, D1), they could also pass through bacterial membranes and directly act on their potential targets such as DNA and ribosomes,[7,8] analogous to nitrofurantoin. The synergistic effect on bacterial killing could lead to a new generation of antibiotics with high potency and novel mechanisms, as well as lower probability of developing resistance. Herein, we report the design, synthesis, and investigation of hydantoin derivatives containing hydrophobic tails and cationic charged groups. Our studies show that these compounds exhibit significantly enhanced antimicrobial activity compared to nitrofurantoin against both Gram-positive and Gram-negative bacteria (>50-fold for certain strains), including clinically relevant multidrug resistant bacterial strains. The lead compound also shows excellent *in vivo* activity toward MRSA-induced pneumonia in a rat model by effectively eradicating MRSA and suppressing lung inflammation caused by pneumonia.

RESULTS AND DISCUSSION

We attempted to design membrane-active hydantoins in a very straightforward manner, thereby making it possible for convenient optimization and production in the future. As shown in Figure 2, R_2 was designated to be the cationic NH_2 group, R_1 was a hydrophobic group, and Cx was a lipid tail. The synthesis was also very straightforward (Figure 3), which allowed a series of compounds to be prepared rapidly on the solid phase. Briefly, the alloc protected γ-AApeptide building block[47,48] bearing the R_2 side chain was attached to Rink-amide resin. After the alloc group was removed, R_1NCO was added to react with the secondary amine to introduce a urea functionality. Next, the Fmoc protecting group was removed, followed by reaction with CxCOCl to introduce the lipid tail. The molecule was then cleaved from the solid support in the presence of 1:1 TFA/DCM, which cyclized spontaneously *in situ* to yield the desired hydantoin product in good yield.

Subsequently, these cationic hydantoin derivatives were tested for their antimicrobial activity against a panel of Gram-positive and Gram-negative bacteria, including multidrug-resistant clinically relevant strains. Compound **26**, nitrofurantoin, exhibited antimicrobial activity

against most of the strains examined, with MICs ranging from 6.25 to 25 μg/mL (Table 1); these values are highly consistent with previously reported antibacterial activity data.[11,49] Although nitrofurantoin is the preferred antibiotic to treat bladder and urinary tract infections, as shown above, its antibacterial activity is moderate. It should also be noted that under the tested conditions, nitrofurantoin failed to show any activity toward *P. aeruginosa*, a notorious Gram-negative strain that can cause severe or even lethal infection.

As a proof of concept, we fixed the cationic R_2 group from the side chain of lysine (Figure 2) and explored the activity of the compounds with respect to the variation of the hydrophobic R_1 group and Cx lipid tail. With an ethyl group for R_1 and a C10 decanoic tail for Cx, compound **1** did not exhibit any activity against all tested bacterial strains. This could be due to insufficient hydrophobicity of the ethyl group and the short length of the lipid tail, rendering compound **1** ineffective to interact with bacteria. It is therefore reasonable that the antimicrobial activities of compounds **2** and **3** increase as their lipid tails become longer, which makes them more membrane active. Indeed, compound **3** already has comparable activity to that of nitrofurantoin against most strains. In addition, it shows an encouraging MIC of 12.5 μg/mL toward *P. aeruginosa*, which is much more potent than nitrofurantoin, suggesting that this class of hydantoin compounds could be further developed. However, it is intriguing that the longer lipid tail does not necessarily lead to more potent antimicrobial agents. For example, compound **4**, which contains the same ethyl group for R_1 but a C16 palmitic tail, exhibited enhanced activity against Gram-positive bacteria, but its activity toward *P. aeruginosa* was abolished. This clearly implies that both the hydantoin core (D1) and membrane interacting domain (D2) are required for good antimicrobial activity and that a balance of hydrophobicity for R_1 and lipid tail length for Cx is needed. Following the preliminary studies on this series of ethyl-containing hydantoins, we set out to test the activity of a few more compounds containing R_1 of increasing hydrophobicity. With enhanced rigidity and hydrophobicity, these compounds with the same lipid tails were generally more active. For instance, compound **5**, containing a butyl group, does not have any antimicrobial activity. In contrast, compound **9**, bearing a cyclohexyl group for R_1, starts to show activity toward a few bacterial strains. Further, compound **13** with an adamantyl group already exhibits decent activity across the panel of bacteria. Similar to compounds **1–4**, in each series of compounds bearing the same R_1 group, increasing the length of the lipid tail led to an initial enhancement and then a detriment in antimicrobial activity. It seems that there is a consistent trend in which compounds containing a C12 or C14 tail possess optimal antimicrobial activity. As aromatic groups are frequently identified in the vast majority of antibiotic agents, we next tested the activity of hydantoins containing phenyl groups as the R_1 group. Although *para*-methoxybenzyl group-containing compounds **17–20** do not yield better antibiotic agents, hydantoins possessing *meta*-chlorobenzyl groups led to new compounds with potent and broad-spectrum activity. The most potent compound, **22**, exhibited MICs less than 1 μg/mL against all tested Gram-positive and Gram-negative strains. Compared with nitrofurantoin, **22** is 25-fold as effective toward MRSA and at least 50-fold more effective toward *P. aeruginosa*. Last, we examined the impact of the cationic charge of R_2 on the antimicrobial activity. Surprisingly, replacement of the cationic aminobutyryl group in **22** with the phenyl group gave the highly hydrophobic compound **25**, which failed to show any antimicrobial activity. This strongly

supports the conclusion that the cationic charge is of vital importance for the antimicrobial activity of this class of hydantoin compounds, possible due to its electrostatic interaction with negatively charged bacterial membranes. In addition, the amphiphilicity of the compounds has to be carefully tuned to result in the optimal interaction with the bacterial membrane. We also evaluated the overall amphiphilicity of molecules based on their HPLC retention time (t_R values). As observed from HPLC data (Table S1 in Supporting Information), no apparent antibacterial activity was displayed when t_R values were less than 26 min (compounds **1, 2, 4, 5, 6, 9, 17, 18**, and **25**). The antibacterial activity in general increased with an increase in the t_R value from 26 to 28.4 min (compound **22**); it then decreased when the t_R value was more than 28.4 min. In order to have antibacterial activity, the compounds must have t_R values between 26 and 29 min.

In order to evaluate the therapeutic potential of these hydantoin compounds, we next investigated the selectivity of the lead compounds that exhibited broad-spectrum antimicrobial activity against all tested strains. As shown in Table 2, these compounds all have better antimicrobial activity than nitrofurantoin **26** while exhibiting limited hemolytic activity. Most noticeably, the most potent compound, **22**, with significantly enhanced activity compared with nitrofurantoin, show excellent selectivity toward MRSA. In addition to hemolytic activity, **22** also showed similar selectivity for mammalian cells, with IC_{50}'s of 90 and 100 μg/mL toward ovarian cancer cells (C13) and colon cancer cells (HCT116), respectively.

As aforementioned, the antimicrobial mechanisms of hydantoins are complex and elusive. However, since the compounds developed here were expected to at least possess a mechanism of action analogous to that of HDPs, their impact on bacterial membranes could be investigated by fluorescent microscopic studies.[44] The most potent compound, **22**, was thus examined for its ability to compromise bacterial membranes of Gram-positive MRSA and Gram-negative *Escherichia coli*.[45] Two dyes, 4′,6-diamidino-2-phenylindole (DAPI) and propidium iodide (PI) (Figure 4), were used to differentiate between cells with either an intact or a damaged membrane. DAPI can permeate the membrane of intact cells and therefore shows blue fluorescence regardless of cell viability. In contrast, PI is a DNA intercalator but lacks cell permeability. It fluoresces in red only when cell membranes are disrupted. As shown in Figure 4, in the DAPI channel, both MRSA and *E. coli* exhibited blue fluorescence (Figure 4a1,a3) in the absence of compound **22**, whereas neither strain showed fluorescence in the PI channel (Figure 4b1,b3), indicating the membranes of these bacteria were intact. However, after bacteria including both MRSA and *E. coli* were incubated with **22** for 2 h, they were stained by both DAPI and PI (Figure 4a2,b2,a4,b4), suggesting that the membranes of both MRSA and *E. coli* were damaged. Nitrofurantoin was also subjected to the same experiment; however, it did not show any membrane-disruption activity even at 100 μg/mL (Figure S2), demonstrating that it does not inhibit bacterial growth through membrane disruption.

HDPs are well-known for their ability to eradicate bacteria rapidly due to their membrane-disruptive bactericidal mechanism.[50] It is of interest to know if our newly synthesized hydantoin compounds exhibit similar bacterial killing kinetics. As such, we subsequently carried out time-kill studies for **22** at different concentrations toward MRSA and *E. coli*. As

shown in Figure 5, at 25 μg/mL, **22** could completely eradicate MRSA in just 10 min (Figure 5a). Even at 2.0 μg/mL (4× MIC), MRSA was thoroughly removed in 60 min. Killing *E. coli* is relatively slower; however, all bacteria were still eradicated in 30 min at 25 or 50 μg/mL. At 4.0 μg/mL (4× MIC), *E. coli* could also be completely eradicated in 60 min. This demonstrates that this class of hydantoin compounds can rapidly kill both Grampositive and Gram-negative pathogens, analogous to HDPs.

One of the most appealing features of HDPs is that they do not readily elicit bacteria resistance, as they disrupt bacterial membranes rather than acting on specific targets.[51] Since compound **22** was designed to be membrane active, in addition to its mechanism of action due to the hydantoin core, we hypothesized that **22** could also prevent the development of resistance in bacteria. As such, we conducted drug resistance studies for **22** against MRSA. **22** was incubated with bacteria at half of its MIC overnight, and the new MIC was measured subsequently. After 14 passages, the MICs of **22** remained virtually unchanged (Figure 6), which strongly suggests that this class of hydantoin compounds does not readily induce resistance in bacteria, thereby augmenting their potential therapeutic applications.

One of the major causes of pneumonia is bacterial infection.[52] Hospital-acquired and community-acquired MRSA pneumonia has become more prevalent in recent years and presents significant therapeutic challenges due to its increasing motility.[52] As our hydantoin compounds exhibited potent *in vitro* antibacterial activity against both Gram-positive and Gram-negative bacteria including MRSA, it was intriguing to investigate their *in vivo* activity to assess their therapeutic potential. As such, we tested their efficacy in a rat model bearing MRSA pneumonia induced by intratracheal instillation.[41,53] As shown in Figure 7, the control group, which was treated with PBS only, exhibited a high level of MRSA after bacterial inoculation. The slightly decreased quantity of bacteria on day 5 compared with day 3 suggested that rats may fight MRSA through their host immune response.[53] However, the impact of this response on bacterial clearance was very minimal. Vancomycin, which has long been considered the “last-resort” antibiotic to treat infections caused by multidrug-resistant Gram-positive pathogens such as MRSA, was included as a positive control. As shown in Figure 7, on day 3 after its administration, vancomycin caused a ~30% reduction in bacteria compared with the control. On day 5, the reduction increased to ~45%. This indicates that vancomycin could help to clear MRSA from the lungs of rats; however, it did not exhibit satisfactory efficacy in the inhibition of MRSA proliferation. On the contrary, compound **22** displayed a significantly superior *in vivo* efficacy in the eradication of MRSA bacteria. On day 3 after treatment with **22**, a ~70% reduction in bacteria was observed. On day 5, compared to the control, MRSA was reduced by 96%. The remarkable potency of **22** relative to the control and vancomycin demonstrates its promising therapeutic potential.

Given the findings that **22** could virtually completely eradiate MRSA bacteria in the lungs of rats, we subsequently conducted pathological analysis to find out if **22** could suppress lung inflammation induced by MRSA. As shown in Figure 8, all three groups (PBS control, vancomycin treatment, and **22** treatment) demonstrated normal conditions right after MRSA inoculation (0 days), which suggests that inflammation has not developed in the lungs. However, the inflammation in the control group elevated rapidly due to the lack of treatment, as seen by the presence of a large population of inflammatory cells including monocytes,

macrophages, neutrophils, eosinophils, etc. (blue spots in H&E staining) on day 5, which is the typical indication of severe lung pneumonia. Rats treated with vancomycin showed some alleviation of this condition due to its ability to inhibit the proliferation of MRSA, which decreased the inflammation. Remarkably, treatment with compound **22** had a much more significant impact on the suppression of lung inflammation. On day 3, only mild inflammation was observed, whereas on day 5, the inflammation was further mitigated and virtually matched normal conditions. These findings, consistent with the above-mentioned MRSA proliferation studies, strongly suggest that compound **22** could be superior to vancomycin as a novel therapeutic strategy to treat MRSA pneumonia.

CONCLUSIONS

In summary, we have reported a new class of hydantoin derivatives as potential antibiotic agents. These molecules, bearing a cationic charge and hydrophobic lipid tail, were designed to be membrane active in bacterial killing. They exhibited significantly more potent antimicrobial activity against a panel of multidrug-resistant Gram-positive and Gram-negative bacteria than the marketed antibiotic nitrofurantoin, a hydantoin derivative. Although the mechanisms of action for hydantoin compounds are known to be complex, our investigation demonstrated that the hydantoin compounds reported here could compromise bacterial membranes and kill bacteria rapidly and that they do not induce resistance in MRSA even after 14 passages, which is similar to HDPs. Moreover, these molecules also exhibited excellent *in vivo* efficacy in a rat model bearing MRSA-induced pneumonia by effectively eradicating MRSA bacteria and suppressing lung inflammation, performing superior to vancomycin. Together with their facile synthesis, these compounds could be an appealing class of antibiotic agents to combat emergent drug resistance. Further optimization of lead compounds and efficacy studies using other *in vivo* models are currently underway.

EXPERIMENTAL SECTION

General Information

Rink-amide MBHA resins (0.7 mmol/g, 200–400 mesh) were purchased from Chem-Impex Int'l Inc. Solvents and other chemicals were ordered from either Fisher Scientific or Sigma-Aldrich and were used without further purification. The ^{1}H NMR spectra were obtained on a Varian Inova 400 instrument. The solid-phase syntheses of all compounds were carried out in a peptide reaction vessel on a Burrell wrist-action shaker. All compounds were analyzed and purified using a Waters Breeze 2 HPLC system under a 215 nm UV detector equipped with both analytical and preparative modules. The desired fractions were lyophilized on a Labcono lyophilizer. The purity of the compounds was determined to be >95% by analytical HPLC. Molar masses of compounds were identified by an Agilent Technologies 6540 UHD accurate-mass Q-TOF LC/MS spectrometer.

Synthesis of Desired Compounds

The synthesis of **22** was as follows. The other compounds were synthesized following a similar procedure as that for **22**. 200 mg of Rink-amide (MBHA) resin (0.14 mmol) was treated with 3 mL of a 20% piperidine/DMF (v/v) solution for 15 min (×2) to remove the

Fmoc protection group, followed by washing with DMF (2 mL × 3) and DCM (2 mL × 3). Attachment of the γ-AApeptide building block to the resin was achieved by adding γ-Lys-BB (238 mg, 0.4 mmol), DIC (101 mg, 114 μL, 0.8 mmol), and HOBt (122 mg, 0.8 mmol) in 3 mL of DMF to the reaction vessel, and the reaction was allowed to shake at room temperature for 3 h. The solution was drained, and the beads were washed with DCM (3 mL × 3) and DMF (3 mL × 3). After that, beads were treated with $Pd(PPh_3)_4$ (24 mg, 0.02 mmol) and $Me_2NH{\cdot}BH_3$ (70 mg, 1.2 mmol) in 3 mL of DCM for 10 min (×2) to remove the alloc protecting group and then washed with DCM (3 mL × 3) and DMF (3 mL × 3). Next, 3-chlorophenyl isocyanate (77 mg, 61 μL, 0.5 mmol) and DIPEA (65 mg, 87 μL, 0.5 mmol) in 3 mL of DCM were added to the resin and allowed to react for 30 min at room temperature; the solution was then drained. After washing with DMF (2 mL × 3) and DCM (2 mL × 3), the beads were treated with 3 mL of a 20% piperidine/DMF (v/v) solution for 15 min (× 2) to remove the Fmoc protection group, followed by washing with DMF (2 mL × 3) and DCM (2 mL × 3). Subsequently, lauric acid (80 mg, 0.4 mmol), DIC (101 mg, 114 μL, 0.8 mmol), and HOBt (122 mg, 0.8 mmol) in 3 mL of DMF were added to the reaction vessel and reacted for 3 h. After the solution was drained, the beads were washed with DMF (2 mL × 3) and DCM (2 mL × 3), followed by incubation with 4 mL of a cocktail of 1:1 TFA/DCM 1:1 (v/v) for 2 h to achieve cleavage and global deprotection of the compound. After the solvent was removed *in vacuo*, the residue was analyzed and purified on the Waters HPLC system; the desired fraction was lyophilized to give pure product **22**, which was subsequently characterized by NMR and MS.

(S)-N-(6-Amino-1-(3-ethyl-2,4-dioxoimidazolidin-1-yl)hexan-2-yl)decanamide (1)—^{1}H NMR (400 MHz, DMSO-d_6) δ 7.73 (brd, 3H), 7.61 (d, J = 8.0 Hz, 1H), 4.01 (d, J = 6.8 Hz, 1H), 3.81–3.89 (m, 2H), 3.33–3.36 (m, 3H), 3.09 (dd, J = 14.0, 4.4 Hz, 1H), 2.65–2.74 (m, 2H), 1.96 (t, J = 16.0 Hz, 2H), 1.31–1.49 (m, 6H), 1.10–1.30 (m, 14H), 1.01 (t, J = 14.4 Hz, 3H), 0.81 (t, J = 16.0 Hz, 3H). ^{13}C NMR (100 MHz, DMSO-d_6) δ 173.0, 170.6, 156.8, 50.3, 46.8, 46.7, 39.1, 35.9, 33.4, 31.6, 31.0, 29.2, 29.1, 29.0, 28.9, 27.0, 25.7, 22.8, 22.5, 14.3, 13.6. HRMS (ESI) $C_{21}H_{40}N_4O_3$ $[M + H]^+$ calcd = 397.3175; found = 397.3176.

(S)-N-(6-Amino-1-(3-ethyl-2,4-dioxoimidazolidin-1-yl)hexan-2-yl)dodecanamide (2)—^{1}H NMR (400 MHz, DMSO-d_6) δ 7.70 (brd, 3H), 7.62 (d, J = 8.8 Hz, 1H), 3.80–4.05 (m, 3H), 3.31–3.36 (m, 3H), 3.03 (dd, J = 14.0, 4.0 Hz, 1H), 2.67–2.75 (m, 2H), 1.97 (t, J = 7.2 Hz, 2H), 1.36–1.49 (m, 6H), 1.10–1.25 (m, 18H), 1.02 (t, J = 7.2 Hz, 3H), 0.82 (t, J = 6.4 Hz, 3H). ^{13}C NMR (100 MHz, DMSO-d_6) δ 173.0, 170.7, 156.8, 50.3, 46.9, 46.7, 36.0, 33.4, 31.7, 31.0, 29.4, 29.4, 29.3, 29.2, 29.1, 29.0, 27.7, 25.7, 22.8, 22.5, 14.3, 13.7. HRMS (ESI) $C_{23}H_{44}N_4O_3$ $[M + H]^+$ calcd = 425.3485; found = 425.3486.

(S)-N-(6-Amino-1-(3-ethyl-2,4-dioxoimidazolidin-1-yl)hexan-2-yl)tetradecanamide (3)—^{1}H NMR (400 MHz, DMSO-d_6) δ 7.75 (brd, 3H), 7.63 (d, J = 8.0 Hz, 1H), 4.02 (d, J = 17.2 Hz, 1H), 3.85 (d, J = 17.2 Hz, 1H), 3.31–3.33 (m, 3H), 3.03 (dd, J = 14.0, 4.0 Hz, 1H), 2.70–2.73 (m, 2H), 1.97 (t, J = 7.2 Hz, 2H), 1.29–1.48 (m, 8H), 1.10–1.24 (m, 22H), 1.02 (t, J = 7.2 Hz, 3H), 0.82 (t, J = 6.4 Hz, 3H). ^{13}C NMR (100 MHz, DMSO-d_6) δ 172.8, 170.7, 156.8, 50.3, 46.9, 46.7, 39.3, 39.1, 36.0, 33.4, 31.7, 31.1, 29.4,

29.3, 29.2, 29.1, 29.0, 27.1, 25.7 22.9, 22.5, 14.4, 13.7. HRMS (ESI) $C_{25}H_{48}N_4O_3$ $[M + H]^+$ calcd = 453.3799; found = 453.3800.

(S)-N-(6-Amino-1-(3-ethyl-2,4-dioxoimidazolidin-1-yl)hexan-2-yl)palmitamide (4)—^{1}H NMR (400 MHz, DMSO-d_6) δ 7.77 (brd, 3H), 7.62 (d, J = 9.2 Hz, 1H), 3.79–4.09 (m, 3H), 3.30–3.37 (m, 3H), 3.08 (dd, J = 14.0, 4.0 Hz, 1H), 2.65–2.75 (m, 2H), 1.96 (t, J = 7.6 Hz, 2H), 1.27–1.53 (m, 6H), 1.03–1.24 (m, 26H), 1.01 (t, J = 7.2 Hz, 3H), 0.81 (t, J = 6.4 Hz, 3H). ^{13}C NMR (100 MHz, DMSO-d_6) δ 172.8, 170.6, 156.8, 50.3, 46.9, 46.7, 39.1, 36.0, 33.4, 31.7, 31.1, 29.5, 29.3, 29.2, 29.1, 29.1, 27.1, 25.7 22.9, 22.5, 14.4, 13.7. HRMS (ESI) $C_{27}H_{52}N_4O_3$ $[M + H]^+$ calcd = 481.4112; found = 481.4110.

(S)-N-(6-Amino-1-(3-butyl-2,4-dioxoimidazolidin-1-yl)hexan-2-yl)decanamide (5)—^{1}H NMR (400 MHz, DMSO-d_6) δ 7.72 (brd, 3H), 7.62 (d, J = 8.8 Hz, 1H), 3.85 (d, J = 17.2 Hz, 2H), 3.26–3.45 (m, 3H), 3.00–3.15 (m, 1H), 2.68–2.73 (m, 2H), 1.96 (t, J = 14.8 Hz, 2H), 1.32–1.52 (m, 8H), 1.10–1.25 (m, 16H), 0.79–0.83 (m, 6H). ^{13}C NMR (100 MHz, DMSO-d_6) δ 173.0, 170.9, 157.0, 50.2, 46.9, 46.7, 39.2, 38.1, 36.0, 31.7, 31.0, 30.1, 29.3, 29.2, 29.1, 29.0, 27.1, 25.7, 22.8, 22.5, 19.7, 14.3 13.8. HRMS (ESI) $C_{23}H_{44}N_4O_3$ $[M + H]^+$ calcd = 425.3486; found = 425.3487.

(S)-N-(6-Amino-1-(3-butyl-2,4-dioxoimidazolidin-1-yl)hexan-2-yl)dodecanamide (6)—^{1}H NMR (400 MHz, DMSO-d_6) δ 7.75 (brd, 3H), 7.62 (d, J = 9.2 Hz, 1H), 4.02 (d, J = 17.2 Hz 1H), 3.82–3.94 (m, 2H), 3.25–3.39 (m, 3H), 3.07 (dd, J = 14.0, 4.0 Hz, 1H), 2.68–2.74 (m, 2H), 1.96 (t, J = 7.6 Hz, 2H), 1.29–1.51 (m, 8H), 1.10–1.22 (m, 20H), 0.79–0.84 (m, 6H). ^{13}C NMR (100 MHz, DMSO-d_6) δ 172.8, 170.8, 156.9, 50.2, 46.9, 46.7, 39.1, 38.1, 36.0, 31.7, 31.1, 30.1, 29.5, 29.4, 29.3, 29.2, 29.1, 27.1, 25.7, 22.9, 22.5, 19.7, 14.4, 13.9. HRMS (ESI) $C_{25}H_{48}N_4O_3$ $[M + H]^+$ calcd = 453.3802; found = 453.3803.

(S)-N-(6-Amino-1-(3-butyl-2,4-dioxoimidazolidin-1-yl)hexan-2-yl)tetradecanamide (7)—^{1}H NMR (400 MHz, DMSO-d_6) δ 7.73 (brd, 3H), 7.62 (d, J = 8.8 Hz, 1H), 4.02 (d, J = 17.6 Hz 1H), 3.82–3.90 (m, 2H), 3.26–3.38 (m, 3H), 3.07 (dd, J = 14.0, 4.0 Hz, 1H), 2.68–2.74 (m, 2H), 1.95 (t, J = 7.2 Hz, 2H), 1.30–1.54 (m, 8H), 1.12–1.25 (m, 24H), 0.78–0.84 (m, 6H). ^{13}C NMR (100 MHz, DMSO-d_6) δ 172.8, 170.8, 156.9, 50.2, 46.9, 46.7, 39.1, 38.1, 36.0, 31.7, 31.1, 30.1, 29.5, 29.3, 29.2, 29.1, 27.1, 25.7, 22.9, 22.5, 19.7, 14.3, 13.9. HRMS (ESI) $C_{27}H_{52}N_4O_3$ $[M + H]^+$ calcd = 481.4112; found = 481.4111.

(S)-N-(6-Amino-1-(3-butyl-2,4-dioxoimidazolidin-1-yl)hexan-2-yl)palmitamide (8)—^{1}H NMR (400 MHz, DMSO-d_6) δ 7.77 (brd, 3H), 7.62 (d, J = 9.2 Hz, 1H), 4.02 (d, J = 17.2 Hz 1H), 3.82–3.89 (m, 2H), 3.25–3.38 (m, 3H), 3.07 (dd, J = 13.6, 4.0 Hz, 1H), 2.68–2.73 (m, 2H), 1.95 (t, J = 7.2 Hz, 2H), 1.27–1.50 (m, 8H), 1.08–1.22 (m, 28H), 0.79–0.84 (m, 6H). ^{13}C NMR (100 MHz, DMSO-d_6) δ 173.0, 170.8, 157.0, 50.1, 46.9, 46.7, 38.1, 36.0, 31.7, 31.1, 30.1, 29.4, 29.3, 29.2, 29.1, 27.1, 25.7, 22.8, 22.5, 19.7, 14.3, 13.8. HRMS (ESI) $C_{29}H_{56}N_4O_3$ $[M + H]^+$ calcd = 509.4422; found = 509.4424.

(S)-N-(6-Amino-1-(3-cyclohexyl-2,4-dioxoimidazolidin-1-yl)-hexan-2-yl)decanamide (9)—^{1}H NMR (400 MHz, DMSO-d_6) δ 7.66 (brd, 3H), 7.59 (d, J = 8.8 Hz, 1H), 3.95–3.98 (m, 1H), 3.73–3.85 (m, 2H), 3.61–3.72 (m, 1H), 3.29–3.35 (m, 1H),

3.03–3.08 (m, 1H), 2.65–2.72 (m, 2H), 1.93–1.98 (m, 4H), 1.72 (d, J = 12.4 Hz, 2H), 1.28–1.57 (m, 8H), 1.02–1.24 (m, 18H), 0.82 (t, J = 6.8 Hz, 3H). ^{13}C NMR (100 MHz, DMSO-d_6) δ 172.9, 170.8, 156.7, 50.9, 49.8, 46.9, 46.6, 36.0, 31.7, 31.0, 29.4, 29.4, 29.2, 29.2, 29.1, 27.1, 25.7, 25.2, 22.8, 22.5, 14.3. HRMS (ESI) $C_{25}H_{46}N_4O_3$ $[M + H]^+$ calcd = 451.3643; found = 451.3644.

(S)-N-(6-Amino-1-(3-cyclohexyl-2,4-dioxoimidazolidin-1-yl)-hexan-2-yl)dodecanamide (10)—^{1}H NMR (400 MHz, DMSO-d_6) δ 7.64 (brd, 3H), 7.60 (d, J = 9.2 Hz, 1H), 3.95–4.05 (m, 3H), 3.34–3.36 (m, 1H), 3.25 (s, 1H), 3.00–3.09 (m, 1H), 2.71 (s, 2H), 1.90–2.00 (m, 4H), 1.72 (d, J = 12.4 Hz, 2H), 1.31–1.59 (m, 8H), 1.00–1.27 (m, 22H), 0.82 (t, J = 6.0 Hz, 3H). ^{13}C NMR (100 MHz, DMSO-d_6) δ 173.2, 170.8, 156.7, 50.9, 49.8, 46.9, 46.6, 36.0, 31.7, 31.1, 29.4, 29.4, 29.3, 29.1, 27.1, 25.8, 25.3, 22.5. HRMS (ESI) $C_{27}H_{50}N_4O_3$ $[M + H]^+$ calcd = 479.3955; found = 479.3956.

(S)-N-(6-Amino-1-(3-cyclohexyl-2,4-dioxoimidazolidin-1-yl)-hexan-2-yl)tetradecanamide (11)—^{1}H NMR (400 MHz, DMSO-d_6) δ 7.72 (brd, 3H), 7.60 (d, J = 9.2 Hz, 1H), 3.92–4.00 (m, 1H), 3.61–3.85 (m, 2H), 3.25–3.36 (m, 2H), 3.01–3.10 (m, 1H), 2.68–2.71 (m, 2H), 1.91–2.01 (m, 4H), 1.72 (d, J = 12.4 Hz, 2H), 1.30–1.58 (m, 8H), 0.98–1.25 (m, 26H), 0.82 (t, J = 6.4 Hz, 3H). ^{13}C NMR (100 MHz, DMSO-d_6) δ 172.7, 170.6, 156.7, 50.9, 49.8, 46.9, 46.6, 39.1, 36.1, 31.7, 31.1, 29.5, 29.4, 29.3, 29.2, 29.1, 27.1, 25.8, 25.2, 22.9, 22.5, 14.3. HRMS (ESI) $C_{29}H_{54}N_4O_3$ $[M + H]^+$ calcd = 507.4269; found = 507.4272.

(S)-N-(6-Amino-1-(3-cyclohexyl-2,4-dioxoimidazolidin-1-yl)-hexan-2-yl)palmitamide (12)—^{1}H NMR (400 MHz, DMSO-d_6) δ 7.77 (brd, 3H), 7.61 (d, J = 9.2 Hz, 1H), 3.96 (d, J = 12.4 Hz, 1H), 3.63–3.81 (m, 2H), 3.28–3.33 (m, 2H), 3.00–3.10 (m, 1H), 2.62–2.75 (m, 2H), 1.91–1.99 (m, 4H), 1.70 (d, J = 12.0 Hz, 2H), 1.31–1.59 (m, 8H), 0.99–1.24 (m, 30H), 0.81 (t, J = 6.4 Hz, 3H). ^{13}C NMR (100 MHz, DMSO-d_6) δ 173.1, 170.7, 156.7, 51.0, 49.8, 46.9, 46.6, 36.1, 31.7, 31.0, 29.4, 29.3, 29.2, 29.1, 27.0, 25.8, 25.2, 22.8, 22.5, 14.3. HRMS (ESI) $C_{31}H_{58}N_4O_3$ $[M + H]^+$ calcd = 535.4582; found = 535.4583.

N-((S)-1-(3-((3R,5R,7R)-Adamantan-1-yl)-2,4-dioxoimidazolidin-1-yl)-6-aminohexan-2-yl)decanamide (13)—^{1}H NMR (400 MHz, DMSO-d_6) δ 7.76 (brd, 3H), 7.58 (d, J = 9.2 Hz, 1H), 3.65–3.88 (m, 3H), 3.26–3.33 (m, 1H), 2.99 (dd, J = 14.0, 4.0 Hz, 1H), 2.68–2.74 (m, 2H), 2.27 (d, J = 2.4 Hz, 6H), 1.93–2.03 (m, 5H), 1.59 (s, 6H), 1.26–1.51 (m, 6H), 1.15–1.23 (m, 14H), 0.81 (t, J = 7.2 Hz, 3H). ^{13}C NMR (100 MHz, DMSO-d_6) δ 172.7, 171.5, 157.3, 59.1, 49.7, 46.7, 46.5, 39.1, 36.2, 36.1, 31.7, 31.2, 29.5, 29.3, 29.2, 27.1, 25.8, 22.9, 22.5, 14.3. HRMS (ESI) $C_{29}H_{50}N_4O_3$ $[M + H]^+$ calcd = 503.3955; found = 503.3955.

N-((S)-1-(3-((3R,5R,7R)-Adamantan-1-yl)-2,4-dioxoimidazolidin-1-yl)-6-aminohexan-2-yl)dodecanamide (14)—^{1}H NMR (400 MHz, DMSO-d_6) δ 7.70 (brd, 3H), 7.57 (d, J = 9.2 Hz, 1H), 3.85 (d, J = 17.2 Hz, 2H), 3.67 (d, J = 17.2 Hz, 1H), 3.26–3.33 (m, 1H), 2.99 (dd, J = 14.0, 4.0 Hz, 1H), 2.66–2.73 (m, 2H), 2.27 (d, J = 2.4 Hz, 6H), 1.95–2.01 (m, 5H), 1.59 (s, 6H), 1.26–1.51 (m, 6H), 1.12–1.23 (m, 18H), 0.81 (t, J = 6.4 Hz, 3H). ^{13}C NMR (100 MHz, DMSO-d_6) δ 172.9, 171.5, 157.3,59.1, 49.6, 46.6, 46.5, 36.2, 36.1,

31.7, 31.2, 29.5, 29.4, 29.3, 29.3, 29.2, 29.1, 27.1, 25.8, 22.9, 22.5 14.3. HRMS (ESI) $C_{31}H_{54}N_4O_3$ $[M + H]^+$ calcd = 531.4269; found = 531.4269.

N-((S)-1-(3-((3R,5R,7R)-Adamantan-1-yl)-2,4-dioxoimidazolidin-1-yl)-6-aminohexan-2-yl)tetradecanamide (15)—^{1}H NMR (400 MHz, DMSO-d_6) δ 7.72 (brd, 3H), 7.57 (d, J = 9.2 Hz, 1H), 3.85 (d, J = 17.2 Hz, 2H), 3.68 (d, J = 17.2 Hz, 1H), 3.27–3.34 (m, 1H), 2.99 (dd, J = 14.0, 4.0 Hz, 1H), 2.66–2.74 (m, 2H), 2.27 (d, J = 2.4 Hz, 6H), 1.94–2.01 (m, 5H), 1.59 (s, 6H), 1.26–1.50 (m, 6H), 1.13–1.22 (m, 22H), 0.81 (t, J = 6.4 Hz, 3H). ^{13}C NMR (100 MHz, DMSO-d_6) δ 172.9, 171.5, 157.3,59.1, 49.6, 46.6, 46.5, 39.1, 36.1, 36.1, 31.7, 31.1, 29.5, 29.4, 29.4, 29.3, 29.3, 29.2, 29.1, 27.1, 25.8, 22.8, 22.5, 14.3. HRMS (ESI) $C_{33}H_{58}N_4O_3$ $[M + H]^+$ calcd = 559.4578; found = 559.4579.

N-((S)-1-(3-((3R,5R,7R)-Adamantan-1-yl)-2,4-dioxoimidazolidin-1-yl)-6-aminohexan-2-yl)palmitamide (16)—^{1}H NMR (400 MHz, DMSO-d_6) δ 7.63 (brd, 3H), 7.57 (d, J = 8.8 Hz, 1H), 3.85 (d, J = 17.2 Hz, 2H), 3.68 (d, J = 17.2 Hz, 1H), 3.25–3.33 (m, 1H), 2.99 (dd, J = 14.0, 4.0 Hz, 1H), 2.68–2.73 (m, 2H), 2.27 (d, J = 2.4 Hz, 6H), 1.92–2.02 (m, 5H), 1.60 (s, 6H), 1.24–1.50 (m, 6H), 1.10–1.20 (m, 26H), 0.81 (t, J = 7.2 Hz, 3H). ^{13}C NMR (100 MHz, DMSO-d_6) δ 172.9, 171.5, 157.3,59.1, 49.6, 46.6, 46.4, 39.1, 36.1, 36.1, 31.7, 31.1, 29.5, 29.4, 29.3, 29.3, 29.2, 29.1, 27.1, 25.8, 22.8, 22.5, 14.3. HRMS (ESI) $C_{35}H_{62}N_4O_3$ $[M + H]^+$ calcd = 587.4895; found = 587.4897.

(S)-N-(6-Amino-1-(3-(4-methoxyphenyl)-2,4-dioxoimidazolidin-1-yl)hexan-2-yl)decanamide (17)—^{1}H NMR (400 MHz, DMSO-d_6) δ 7.74 (brd, 3H), 7.68 (d, J = 8.8 Hz, 1H), 7.16 (d, J = 9.2 Hz, 2H), 6.97 (d, J = 8.8 Hz, 2H), 4.18 (d, J = 17.2 Hz, 1H), 3.92–4.03 (m, 2H), 3.74 (s, 3H), 3.36–3.42 (m, 1H), 3.17 (dd, J = 14.0, 4.0 Hz, 1H), 2.68–2.76 (m, 2H), 1.99 (t, J = 7.2 Hz, 2H), 1.29–1.54 (m, 6H), 1.06–1.25 (m, 14H), 0.80 (t, J = 6.0 Hz, 3H). ^{13}C NMR (100 MHz, DMSO-d_6) δ 173.1, 170.1, 159.0, 156.2, 128.2, 125.2, 114.4, 55.8, 50.4, 47.2, 46.8, 36.1, 31.7, 31.0, 29.3, 29.1, 27.1, 25.8, 22.9, 22.5, 14.4. HRMS (ESI) $C_{26}H_{42}N_4O_3$ $[M + H]^+$ calcd = 475.3279; found = 475.3279.

(S)-N-(6-Amino-1-(3-(4-methoxyphenyl)-2,4-dioxoimidazolidin-1-yl)hexan-2-yl)dodecanamide (18)—^{1}H NMR (400 MHz, DMSO-d_6) δ 7.78 (brd, 3H), 7.68 (d, J = 8.8 Hz, 1H), 7.16 (d, J = 9.2 Hz, 2H), 6.96 (d, J = 9.2 Hz, 2H), 4.18 (d, J = 17.2 Hz, 1H), 3.90–4.03 (m, 2H), 3.74 (s, 3H), 3.37–3.43 (m, 1H), 3.13–3.20 (m, 1H), 2.65–2.80 (m, 2H), 1.99 (t, J = 7.2 Hz, 2H), 1.29–1.53 (m, 6H), 1.07–1.24 (m, 18H), 0.80 (t, J = 6.0 Hz, 3H). ^{13}C NMR (100 MHz, DMSO-d_6) δ 173.1, 170.0, 158.9, 156.2, 128.2, 125.2, 114.5, 55.7, 50.4, 47.2, 46.8, 39.1, 36.0, 31.7, 31.0, 29.5, 29.4, 29.3, 29.2, 29.1, 27.1, 25.8, 22.8, 22.5, 14.3. HRMS (ESI) $C_{28}H_{46}N_4O_3$ $[M + H]^+$ calcd = 503.3592; found = 503.3594.

(S)-N-(6-Amino-1-(3-(4-methoxyphenyl)-2,4-dioxoimidazolidin-1-yl)hexan-2-yl)tetradecanamide (19)—^{1}H NMR (400 MHz, DMSO-d_6) δ 7.77 (brd, 3H), 7.68 (d, J = 9.2 Hz, 1H), 7.16 (d, J = 9.2 Hz, 2H), 6.97 (d, J = 9.2 Hz, 2H), 4.19 (d, J = 17.2 Hz, 1H), 3.91–4.03 (m, 2H), 3.74 (s, 3H), 3.37–3.43 (m, 1H), 3.15–3.21 (m, 1H), 2.70–2.76 (m, 2H), 2.00 (t, J = 7.2 Hz, 2H), 1.30–1.57 (m, 6H), 1.10–1.24 (m, 22H), 0.82 (t, J = 6.4 Hz, 3H). ^{13}C NMR (100 MHz, DMSO-d_6) δ 172.9, 170.0, 159.0, 156.2, 128.2, 125.3, 114.4, 55.8,

50.4, 47.2, 46.7, 39.1, 36.1, 31.7, 31.1, 29.5, 29.5, 29.4, 29.3, 29.1, 27.1, 25.8, 22.9, 22.5, 14.4. HRMS (ESI) $C_{23}H_{44}N_4O_3$ $[M + H]^+$ calcd = 531.3896; found = 531.3894.

(S)-N-(6-Amino-1-(3-(4-methoxyphenyl)-2,4-dioxoimidazolidin-1-yl)hexan-2-yl)palmitamide (20)—^{1}H NMR (400 MHz, DMSO-d_6) δ 7.76 (brd, 3H), 7.68 (d, J = 9.2 Hz, 1H), 7.15 (d, J = 9.2 Hz, 2H), 6.96 (d, J = 9.2 Hz, 2H), 4.18 (d, J = 17.2 Hz, 1H), 3.88–4.04 (m, 2H), 3.73 (s, 3H), 3.39–3.43 (m, 1H), 3.14–3.20 (m, 1H), 2.65–2.78 (m, 2H), 1.99 (t, J = 7.2 Hz, 2H), 1.29–1.53 (m, 6H), 1.10–1.24 (m, 26H), 0.81 (t, J = 6.4 Hz, 3H). ^{13}C NMR (100 MHz, DMSO-d_6) δ 173.1, 170.0, 158.9, 156.2, 128.2, 125.2, 114.3, 55.7, 50.4, 47.2, 46.7, 39.1, 36.0, 31.7, 31.0, 29.4, 29.4, 29.3, 29.2, 29.1, 27.1, 25.8, 22.8, 22.5, 14.3. HRMS (ESI) $C_{32}H_{54}N_4O_3$ $[M + H]^+$ calcd = 559.4218; found = 559.4217.

(S)-N-(6-Amino-1-(3-(3-chlorophenyl)-2,4-dioxoimidazolidin-1-yl)hexan-2-yl)decanamide (21)—^{1}H NMR (400 MHz, DMSO-d_6) δ 7.74 (brd, 3H), 7.69 (d, J = 8.8 Hz, 1H), 7.29–7.50 (m, 4H), 4.01–4.25 (m, 2H), 3.32–3.47 (m, 2H), 3.13–3.21 (m, 1H), 2.73 (s, 2H), 1.99 (t, J = 7.2 Hz, 2H), 1.26–1.51 (m, 8H), 1.05–1.21 (m, 12H), 0.78 (t, J = 6.4 Hz, 3H). ^{13}C NMR (100 MHz, DMSO-d_6) δ 173.0, 169.6, 155.4, 134.0, 133.2, 130.8, 128.0, 126.3, 125.2, 50.4, 47.3, 46.6, 36.0, 31.7, 31.0, 29.3, 29.1, 27.1, 25.8, 22.9, 22.5, 14.4. HRMS (ESI) $C_{25}H_{39}N_4O_3$ $[M + H]^+$ calcd = 479.2779; found = 479.2782.

(S)-N-(6-Amino-1-(3-(3-chlorophenyl)-2,4-dioxoimidazolidin-1-yl)hexan-2-yl)dodecanamide (22)—^{1}H NMR (400 MHz, DMSO-d_6) δ 7.72 (brd, 3H), 7.31–7.49 (m, 4H), 3.98–4.26 (m, 3H), 3.41–3.45 (m, 1H), 3.19–3.22 (m, 1H), 2.74 (s, 2H), 2.01 (s, 2H), 1.35–1.60 (m, 6H), 1.05–1.34 (m, 18H), 0.83 (t, J = 6.8 Hz, 3H). ^{13}C NMR (100 MHz, DMSO-d_6) δ 173.0, 169.8, 155.6, 134.0, 133.2, 130.8, 128.0, 126.3, 125.2, 50.4, 47.3, 46.6, 39.1, 36.0, 31.7, 31.0, 29.5, 29.4, 29.3, 29.3, 29.1, 27.1, 25.8, 22.9, 22.5, 14.4. HRMS (ESI) $C_{27}H_{43}N_4O_3$ $[M + H]^+$ calcd = 507.3092; found = 507.3095

(S)-N-(6-Amino-1-(3-(3-chlorophenyl)-2,4-dioxoimidazolidin-1-yl)hexan-2-yl)tetradecanamide (23)—^{1}H NMR (400 MHz, DMSO-d_6) δ 7.69–7.73 (m, 1H), 7.67 (brd, 3H), 7.15–7.50 (m, 4H), 3.87–4.28 (m, 3H), 3.34–3.45 (m, 1H), 3.13–3.25 (m, 1H), 2.72 (s, 2H), 1.91–2.15 (m, 2H), 1.27–1.49 (m, 6H), 1.09–1.20 (m, 22H), 0.81 (t, J = 6.4 Hz, 3H). ^{13}C NMR (100 MHz, DMSO-d_6) δ 173.2, 169.6, 155.4, 133.9, 133.2, 130.8, 128.0, 126.3, 125.2, 50.3, 47.2, 46.6, 39.1, 36.0, 31.7, 31.0, 29.4, 29.2, 29.2, 29.1, 27.0, 25.8, 22.8, 22.5, 14.3. HRMS (ESI) $C_{29}H_{47}N_4O_3$ $[M + H]^+$ calcd = 535.3408; found = 535.3410.

(S)-N-(6-Amino-1-(3-(3-chlorophenyl)-2,4-dioxoimidazolidin-1-yl)hexan-2-yl)palmitamide (24)—^{1}H NMR (400 MHz, DMSO-d_6) δ 7.67 (d, J = 8.8 Hz, 1H), 7.63 (brd, 3H), 7.28–7.49 (m, 4H), 3.90–4.24 (m, 2H), 3.33–3.44 (m, 2H), 3.15–3.21 (m, 1H), 2.72 (s, 2H), 1.99 (m, J = 7.6 Hz, 2H), 1.30–1.52 (m, 6H), 1.10–1.22 (m, 26H), 0.81 (t, J = 6.4 Hz, 3H). ^{13}C NMR (100 MHz, DMSO-d_6) δ 173.1, 169.6, 155.4, 133.9, 133.2, 130.8, 128.0, 126.3, 125.2, 50.4, 47.2, 46.6, 39.2, 36.0, 31.7, 31.0, 29.4, 29.4, 29.3, 29.2, 29.1, 27.1, 25.8, 22.9, 22.5, 14.4. HRMS (ESI) $C_{31}H_{51}N_4O_3$ $[M + H]^+$ calcd = 563.3722; found = 563.3723.

(S)-N-(1-(3-(3-Chlorophenyl)-2,4-dioxoimidazolidin-1-yl)-3-phenylpropan-2-yl)dodecanamide (25)—^{1}H NMR (400 MHz, DMSO-d_6) δ 7.79 (d, J = 9.2 Hz, 1H), 7.36–7.50 (m, 3H), 7.30 (d, J = 8.0 Hz, 1H), 7.22 (d, J = 4.4 Hz, 4H), 7.10–7.17 (m, 1H), 4.18–4.27 (m, 2H), 4.04 (d, J = 17.6 Hz, 1H), 3.47–3.54 (m, 1H), 3.31–3.27 (m, 1H), 2.76–2.82 (m, 1H), 2.60–2.68 (m, 1H), 1.82–1.95 (m, 2H), 1.02–1.32 (m, 18H), 0.81 (t, J = 6.8 Hz, 3H). ^{13}C NMR (100 MHz, DMSO-d_6) δ 172.8, 169.6, 155.5, 138.9, 134.0, 133.2, 130.8, 129.4, 128.5, 128.0, 126.5, 126.4, 125.3, 50.4, 48.5, 47.2, 40.8, 37.7, 36.0, 31.7, 29.4, 29.4, 29.2, 29.1, 28.9, 25.7, 22.5, 14.4. HRMS (ESI) $C_{31}H_{51}N_4O_3$ $[M + H]^+$ calcd = 526.2826; found = 526.2849.

Supplementary Material

Refer to Web version on PubMed Central for supplementary material.

Acknowledgments

This work was supported by NSF CAREER 1351265 (J.C.), NIH 1RO1GM112652A1 (J.C.), and the Industry-University-Research Collaboration project of Jiangsu Province (BY2015041-01, Y.H.).

ABBREVIATIONS USED

MRSA	methicillin-resistant *Staphylococcus aureus*
MRSE	methicillin-resistant *Staphylococcus epidermidis*
VRE	vancomycin-resistant *Enterococci*
E. coli	*Escherichia coli*
K. P.	*Klebsiella pneumoniae*
P. A.	*Pseudomonas aeruginosa*
HDPs	host-defense peptides
MIC	minimum inhibitory concentration
DAPI	4′,6-diamidino-2-phenylindole
PI	propidium iodide
PBS	phosphate-buffered saline
CFU	colony-forming unit
DMF	dimethylformamide
DCM	dichloromethane
HOBt	hydroxybenzotriazole
DIPEA	*N,N*-diisopropylethylamine
DIC	*N,N′*-diisopropylcarbodiimide

TFA trifluoroacetic acid

References

1. Levy SB, Marshall B. Antibacterial resistance worldwide: causes, challenges and responses. Nat. Med. 2004; 10:S122–129. [PubMed: 15577930]
2. Niku-Paavola ML, Laitila A, Mattila-Sandholm T, Haikara A. New types of antimicrobial compounds produced by lactobacillus plantarum. J. Appl. Microbiol. 1999; 86:29–35. [PubMed: 10200070]
3. Hidayat I-W, Thu YY, Black DSC, Read RW. Biological evaluation of certain substituted hydantoins and benzalhydantoins against microbes. IOP Conf. Ser.: Mater. Sci. Eng. 2016; 107:012058.
4. Fujisaki F, Toyofuku K, Egami M, Ishida S, Nakamoto N, Kashige N, Miake F, Sumoto K. Antibacterial activity of some 5-dialkylaminomethylhydantoins and related derivatives. Chem. Pharm. Bull. 2013; 61:1090–1093. [PubMed: 24088702]
5. Szymanska E, Kiec-Kononowicz K, Bialecka A, Kasprowicz A. Antimicrobial activity of 5-arylidene aromatic derivatives of hydantoin. Part 2. Farmaco. 2002; 57:39–44. [PubMed: 11902644]
6. van der Stelt C, Hofman PS, Nauta WT. The effect of alkyl substitution in drugs. 18. Investigation into the synthesis and antimicrobial properties of 1-[(5-nitrofurfurylidene)amino]hydantoin and its 3-substituted products. A Arzneimittelforschung. 1967; 17:1331–1333. [PubMed: 4885306]
7. Yu T, McCalla DR. Effect of nitrofurazone on bacterial RNA and ribosome synthesis and on the function of ribosomes. Chem.-Biol. Interact. 1976; 14:81–91. [PubMed: 782735]
8. Tu Y, McCalla DR. Effect of activated nitrofurans on DNA. Biochim. Biophys. Acta, Nucleic Acids Protein Synth. 1975; 402:142–149.
9. McOsker CC, Fitzpatrick PM. Nitrofurantoin: mechanism of action and implications for resistance development in common uropathogens. J. Antimicrob. Chemother. 1994; 33:23–30. [PubMed: 7928834]
10. Front Matter A2 - Blass, Benjamin E. Basic Principles of Drug Discovery and Development. Academic Press; Boston: 2015. p. iii
11. Zhanel GG, Hoban DJ, Karlowsky JA. Nitrofurantoin is active against vancomycin-resistant enterococci. Antimicrob. Agents Chemother. 2001; 45:324–326. [PubMed: 11120989]
12. Yu H, Pan L, Li P, Zhang K, Lin X, Zhang Y, Tang X. Nitrofurantoin enteric pellets with high bioavailability based on aciform crystalline formation by wet milling. Pharm. Dev. Technol. 2015; 20:433–441. [PubMed: 24467214]
13. Topcu Y, Tufan F, Bahat G, Karan A. Nitrofurantoin and older women. Can. Med. Assoc. J. 2015; 187:1236.
14. Singh N, Gandhi S, McArthur E, Moist L, Jain AK, Liu AR, Sood MM, Garg AX. Kidney function and the use of nitrofurantoin to treat urinary tract infections in older women. Can. Med. Assoc. J. 2015; 187:648–656. [PubMed: 25918178]
15. Zykov IN, Sundsfjord A, Smabrekke L, Samuelsen O. The antimicrobial activity of mecillinam, nitrofurantoin, temocillin and fosfomycin and comparative analysis of resistance patterns in a nationwide collection of ESBL-producing Escherichia coli in Norway 2010–2011. Infect. Dis. (Lond). 2016; 48(2):99–107. [PubMed: 26414659]
16. Price JR, Guran LA, Gregory WT, McDonagh MS. Nitrofurantoin vs other prophylactic agents in reducing recurrent urinary tract infections in adult women: a systematic review and meta-analysis. Am. J. Obstet. Gynecol. 2016; 215:548–560. [PubMed: 27457111]
17. McKinnell JA, Stollenwerk NS, Jung CW, Miller LG. Nitrofurantoin compares favorably to recommended agents as empirical treatment of uncomplicated urinary tract infections in a decision and cost analysis. Mayo Clin. Proc. 2011; 86:480–488. [PubMed: 21576512]
18. Garau J. Other antimicrobials of interest in the era of extended-spectrum beta-lactamases: fosfomycin, nitrofurantoin and tigecycline. Clin. Microbiol. Infect. 2008; 14:198–202. [PubMed: 18154548]
19. Otreebska-Machaj E, Chevalier J, Handzlik J, Szymanska E, Schabikowski J, Boyer G, Bolla JM, Kiec-Kononowicz K, Pages JM, Alibert S. Efflux pump blockers in gram-negative bacteria: the

new generation of hydantoin based-modulators to improve antibiotic activity. Front. Microbiol. 2016; 7:622. [PubMed: 27199950]

20. Marinova P, Marinov M, Kazakova M, Feodorova Y, Slavchev A, Blazheva D, Georgiev D, Penchev P, Sarafian V, Stoyanov N. Study on the synthesis, characterization and bioactivities of 3-methyl-9′-fluorenespiro-5-hydantoin. Acta. Chim. Slov. 2016; 63:26–32. [PubMed: 26970785]
21. Handzlik J, Szymanska E, Chevalier J, Otrebska E, Kiec-Kononowicz K, Pages JM, Alibert S. Amine-alkyl derivatives of hydantoin: new tool to combat resistant bacteria. Eur. J. Med. Chem. 2011; 46:5807–5816. [PubMed: 22000919]
22. Marr AK, Gooderham WJ, Hancock RE. Antibacterial peptides for therapeutic use: obstacles and realistic outlook. Curr. Opin. Pharmacol. 2006; 6:468–472. [PubMed: 16890021]
23. Hancock RE, Sahl HG. Antimicrobial and host-defense peptides as new anti-infective therapeutic strategies. Nat. Biotechnol. 2006; 24:1551–1557. [PubMed: 17160061]
24. Liu RH, Chen XY, Falk SP, Mowery BP, Karlsson AJ, Weisblum B, Palecek SP, Masters KS, Gellman SH. Structure-activity relationships among antifungal nylon-3 polymers: identification of materials active against drug-resistant strains of candida albicans. J. Am. Chem. Soc. 2014; 136:4333–4342. [PubMed: 24606327]
25. Choi H, Chakraborty S, Liu RH, Gellman SH, Weisshaar JC. Medium effects on minimum inhibitory concentrations of nylon-3 polymers against E-coli. PLoS One. 2014; 9:e104500. [PubMed: 25153714]
26. Raguse TL, Porter EA, Weisblum B, Gellman SH. Structure-activity studies of 14-helical antimicrobial beta-peptides: probing the relationship between conformational stability and antimicrobial potency. J. Am. Chem. Soc. 2002; 124:12774–12785. [PubMed: 12392424]
27. Violette A, Fournel S, Lamour K, Chaloin O, Frisch B, Briand JP, Monteil H, Guichard G. Mimicking helical antibacterial peptides with nonpeptidic folding oligomers. Chem. Biol. 2006; 13:531–538. [PubMed: 16720274]
28. Kapoor R, Eimerman PR, Hardy JW, Cirillo JD, Contag CH, Barron AE. Efficacy of antimicrobial peptoids against Mycobacterium tuberculosis. Antimicrob. Agents Chemother. 2011; 55(6):3058–3062. [PubMed: 21464254]
29. Ghosh C, Manjunath GB, Akkapeddi P, Yarlagadda V, Hoque J, Uppu DS, Konai MM, Haldar J. Small molecular antibacterial peptoid mimics: the simpler the better! J. Med. Chem. 2014; 57:1428–1436. [PubMed: 24479371]
30. Teng P, Shi Y, Sang P, Cai J. γ-AApeptides as a new class of peptidomimetics. Chem. - Eur. J. 2016; 22:5458–5466. [PubMed: 26945679]
31. Shi Y, Teng P, Sang P, She F, Wei L, Cai J. γ-AApeptides: design, structure, and applications. Acc. Chem. Res. 2016; 49:428–441. [PubMed: 26900964]
32. Fjell CD, Hiss JA, Hancock REW, Schneider G. Designing antimicrobial peptides: form follows function. Nat. Rev. Neurosci. 2012; 11:37–51.
33. Hancock REW, Brown KL, Mookherjee N. Host defence peptides from invertebrates - emerging antimicrobial strategies. Immunobiology. 2006; 211:315–322. [PubMed: 16697922]
34. Brown KL, Hancock REW. Cationic host defense (antimicrobial) peptides. Curr. Opin. Immunol. 2006; 18:24–30. [PubMed: 16337365]
35. Choi S, Isaacs A, Clements D, Liu D, Kim H, Scott RW, Winkler JD, DeGrado WF. De novo design and in vivo activity of conformationally restrained antimicrobial arylamide foldamers. Proc. Natl. Acad. Sci. U. S. A. 2009; 106:6968–6973. [PubMed: 19359494]
36. Chongsiriwatana NP, Patch JA, Czyzewski AM, Dohm MT, Ivankin A, Gidalevitz D, Zuckermann RN, Barron AE. Peptoids that mimic the structure, function, and mechanism of helical antimicrobial peptides. Proc. Natl. Acad. Sci. U. S. A. 2008; 105:2794–2799. [PubMed: 18287037]
37. Wu G, Abraham T, Rapp J, Vastey F, Saad N, Balmir E. Daptomycin: evaluation of a high-dose treatment strategy. Int. J. Antimicrob. Agents. 2011; 38:192–196. [PubMed: 21549573]
38. Muraih JK, Pearson A, Silverman J, Palmer M. Oligomerization of daptomycin on membranes. Biochim. Biophys. Acta, Biomembr. 2011; 1808:1154–1160.
39. Yahav D, Farbman L, Leibovici L, Paul M. Colistin: new lessons on an old antibiotic. Clin. Microbiol. Infect. 2012; 18:18–29. [PubMed: 22168320]

40. Nation RL, Li J. Colistin in the 21st century. Curr. Opin. Infect. Dis. 2009; 22:535–543. [PubMed: 19797945]
41. Teng P, Huo D, Nimmagadda A, Wu J, She F, Su M, Lin X, Yan J, Cao A, Xi C, Hu Y, Cai J. Small antimicrobial agents based on acylated reduced amide scaffold. J. Med. Chem. 2016; 59:7877–7887. [PubMed: 27526720]
42. Li Y, Smith C, Wu H, Teng P, Shi Y, Padhee S, Jones T, Nguyen AM, Cao C, Yin H, Cai J. Short antimicrobial lipo-alpha/gamma-AA hybrid peptides. ChemBioChem. 2014; 15:2275–2280. [PubMed: 25169879]
43. Padhee S, Li Y, Cai J. Activity of lipo-cyclic gamma-AApeptides against biofilms of Staphylococcus epidermidis and Pseudomonas aeruginosa. Bioorg. Med. Chem. Lett. 2015; 25:2565–2569. [PubMed: 25977094]
44. Li Y, Smith C, Wu H, Padhee S, Manoj N, Cardiello J, Qiao Q, Cao C, Yin H, Cai J. Lipidated cyclic γ-AApeptides display both antimicrobial and anti-inflammatory activity. ACS Chem. Biol. 2014; 9:211–217. [PubMed: 24144063]
45. Niu Y, Padhee S, Wu H, Bai G, Qiao Q, Hu Y, Harrington L, Burda WN, Shaw LN, Cao C, Cai J. Lipogamma-AApeptides as a new class of potent and broad-spectrum antimicrobial agents. J. Med. Chem. 2012; 55:4003–4009. [PubMed: 22475244]
46. Hu Y, Amin MN, Padhee S, Wang RE, Qiao Q, Bai G, Li Y, Mathew A, Cao C, Cai J. Lipidated peptidomimetics with improved antimicrobial activity. ACS Med. Chem. Lett. 2012; 3:683–686. [PubMed: 24900530]
47. Wu HF, She FY, Gao WY, Prince A, Li YQ, Wei LL, Mercer A, Wojtas L, Ma SQ, Cai JF. The synthesis of head-to-tail cyclic sulfono-gamma-AApeptides. Org. Biomol. Chem. 2015; 13:672–676. [PubMed: 25420701]
48. Wu HF, Teng P, Cai JF. Rapid access to multiple classes of peptidomimetics from common gamma-AApeptide building blocks. Eur. J. Org. Chem. 2014; 2014:1760–1765.
49. Chamberlain RE. Chemotherapeutic properties of prominent nitrofurans. J. Antimicrob. Chemother. 1976; 2(4):325–336. [PubMed: 802123]
50. Ge Y, MacDonald DL, Holroyd KJ, Thornsberry C, Wexler H, Zasloff M. In vitro antibacterial properties of pexiganan, an analog of magainin. Antimicrob. Agents Chemother. 1999; 43:782–788. [PubMed: 10103181]
51. Bowdish DME, Davidson DJ, Lau YE, Lee K, Scott MG, Hancock REW. Impact of LL-37 on anti-infective immunity. J. Leukocyte Biol. 2004; 77:451–459. [PubMed: 15569695]
52. Rubinstein E, Kollef MH, Nathwani D. Pneumonia caused by methicillin-resistant Staphylococcus aureus. Clin. Infect. Dis. 2008; 46:S378–385. [PubMed: 18462093]
53. Huo D, Ding J, Cui YX, Xia LY, Li H, He J, Zhou ZY, Wang HW, Hu Y. X-ray CT and pneumonia inhibition properties of gold-silver nanoparticles for targeting MRSA induced pneumonia. Biomaterials. 2014; 35:7032–7041. [PubMed: 24836950]

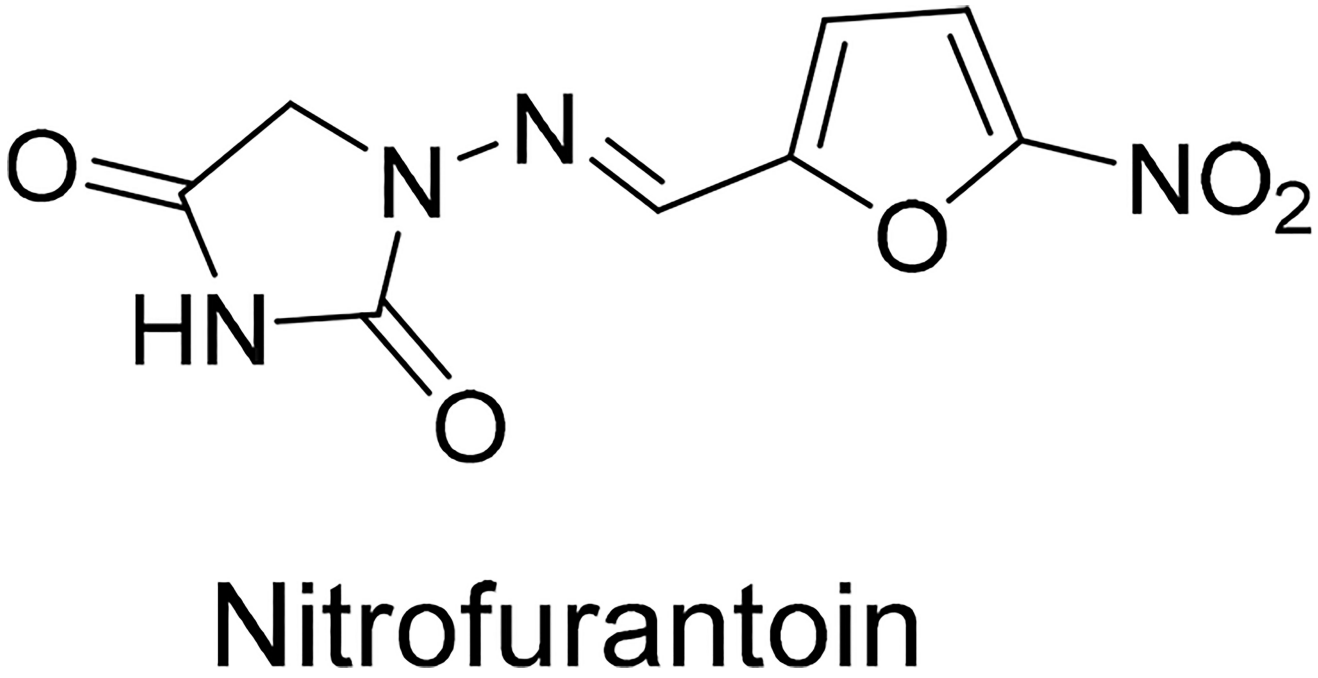

Nitrofurantoin

Figure 1.
Structure of nitrofurantoin.

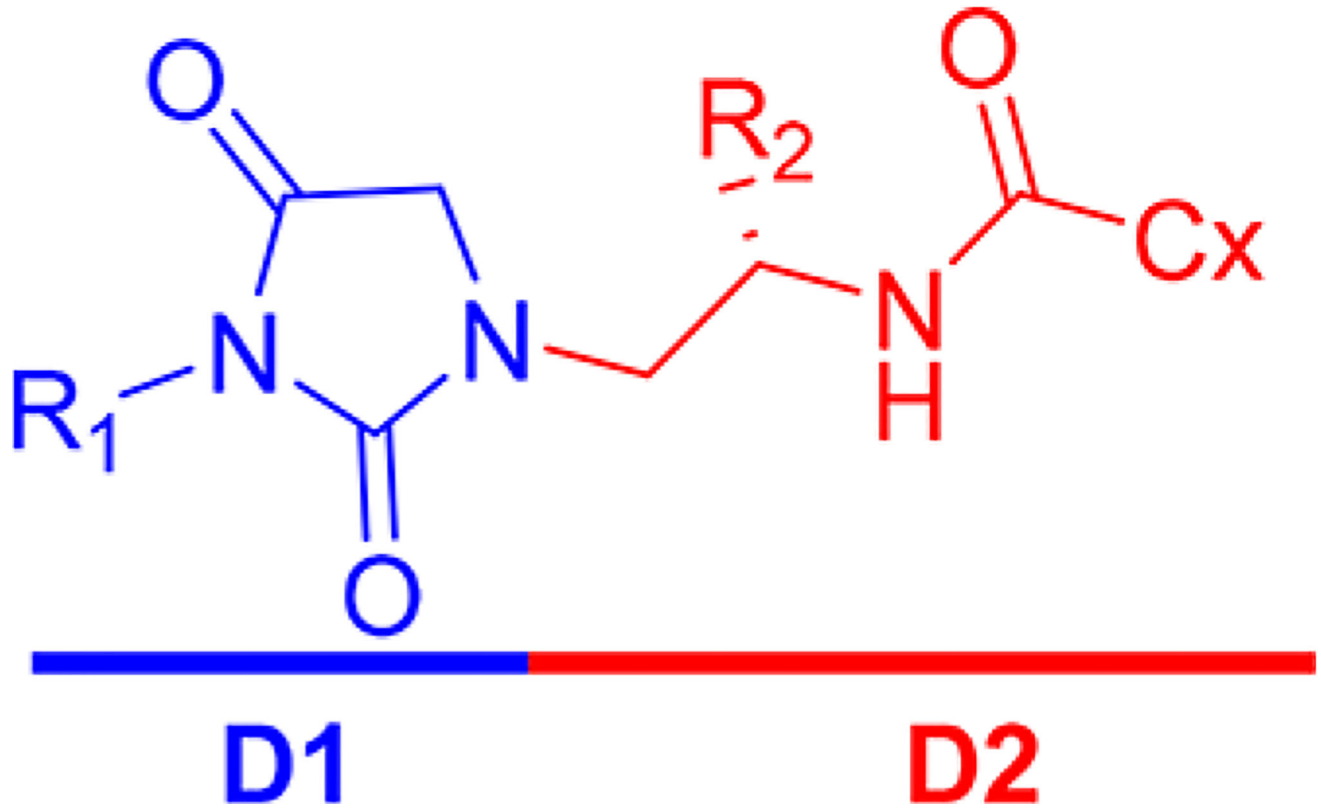

Figure 2.

Design of hydantoin compounds with membrane-acting capability. D1, the hydantoin core, in which R_1 represents a hydrophobic group; D2, membrane interacting domain, in which R_2 is the cationic group. Cx represents lipid tails.

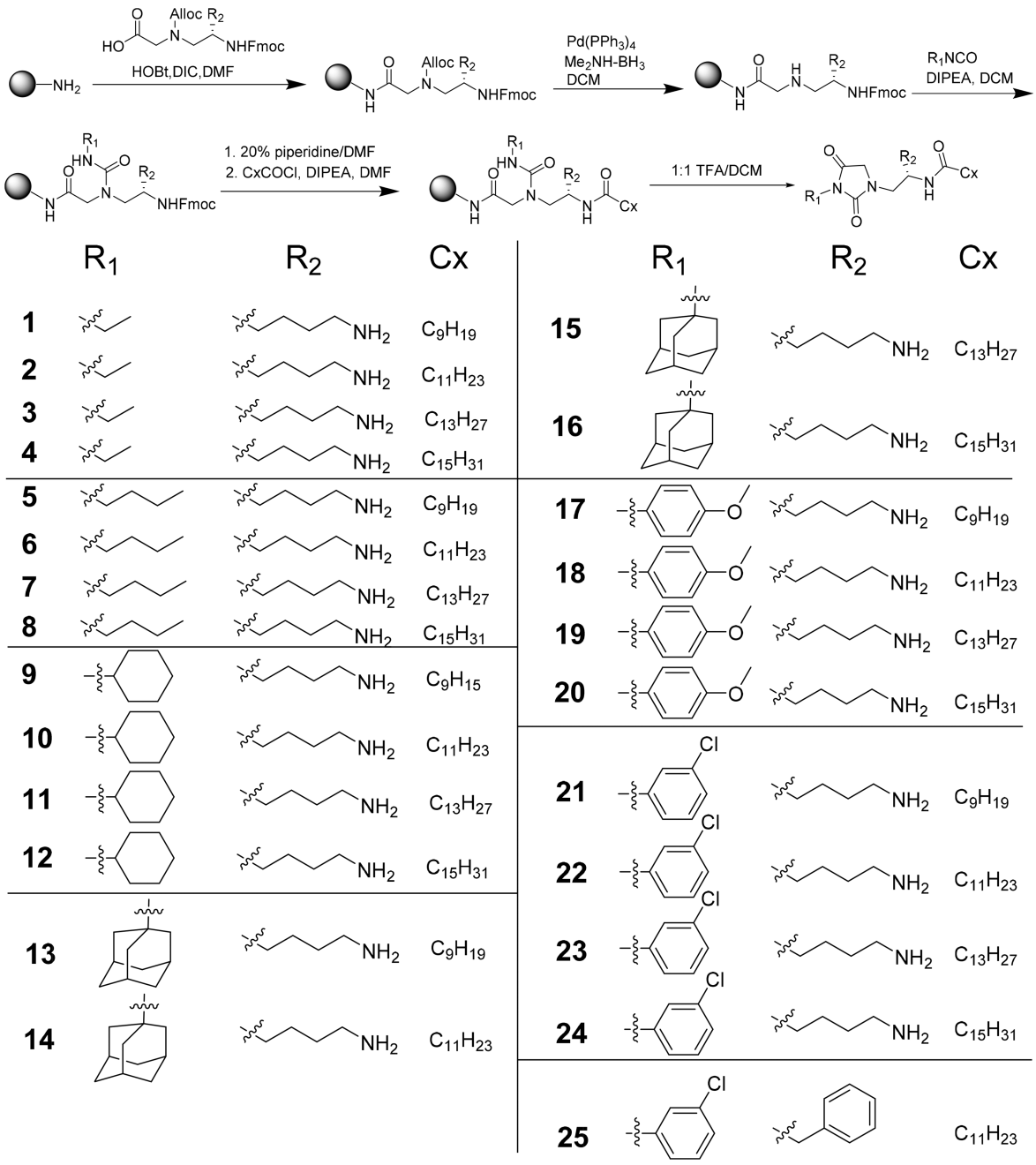

Figure 3.
General approach to synthesize cationic lipidated hydantoins and their structures.

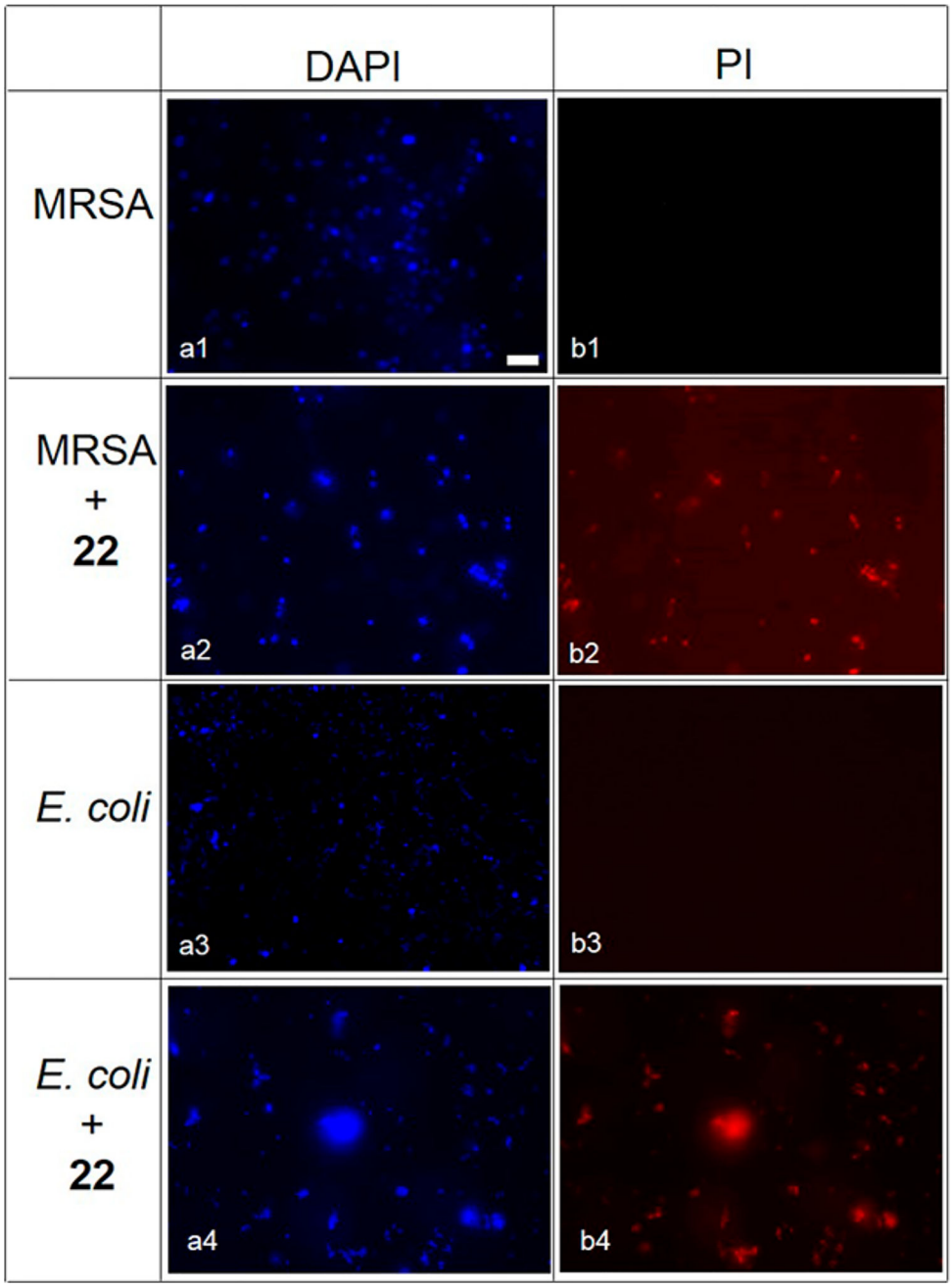

Figure 4.

Fluorescence micrographs of MRSA and *E. coli* treated or not treated with 5 μg/mL **22** for 2 h. (a1) Control, no treatment, DAPI stained; (b1) control, no treatment, PI stained. (a2) MRSA treatment with **22**, DAPI stained; (b2) MRSA treatment with **22**, PI stained. (a3) Control, no treatment, DAPI stained; (b3) control, no treatment, PI stained. (a4) *E. coli* treatment with **22**, DAPI stained; (b4) *E. coli* treatment with **22**, PI stained. Scale bar = 10 μm.

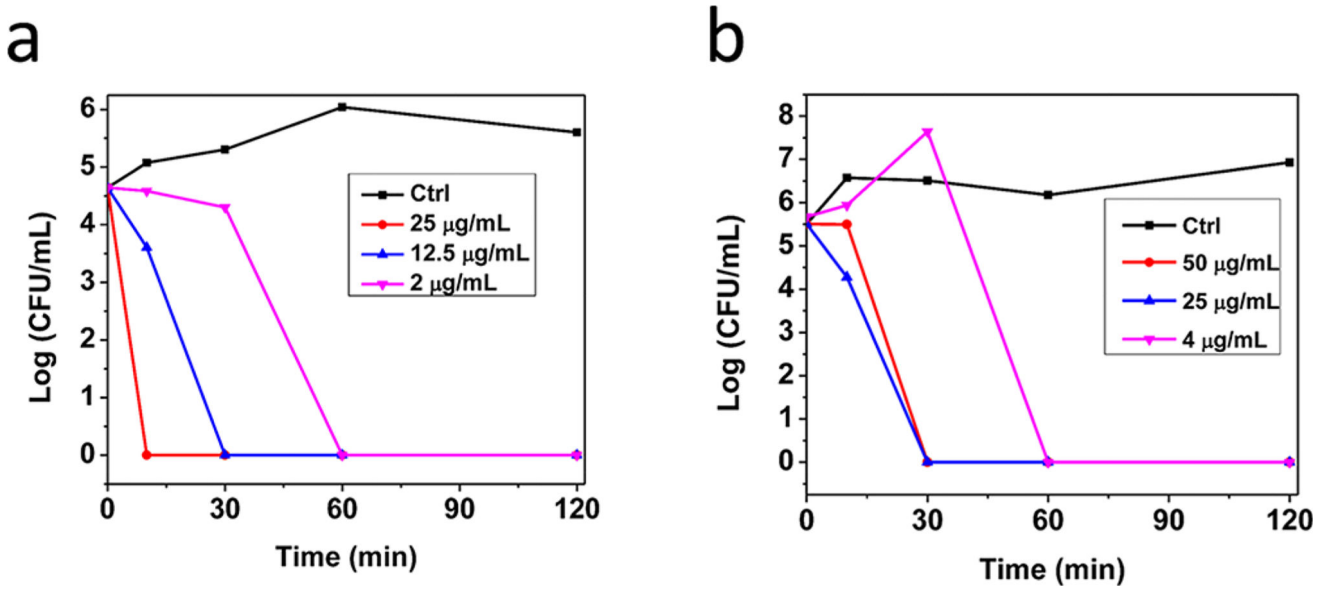

Figure 5.
Time-kill plots of **22** against MRSA (a) and *E. coli* (b).

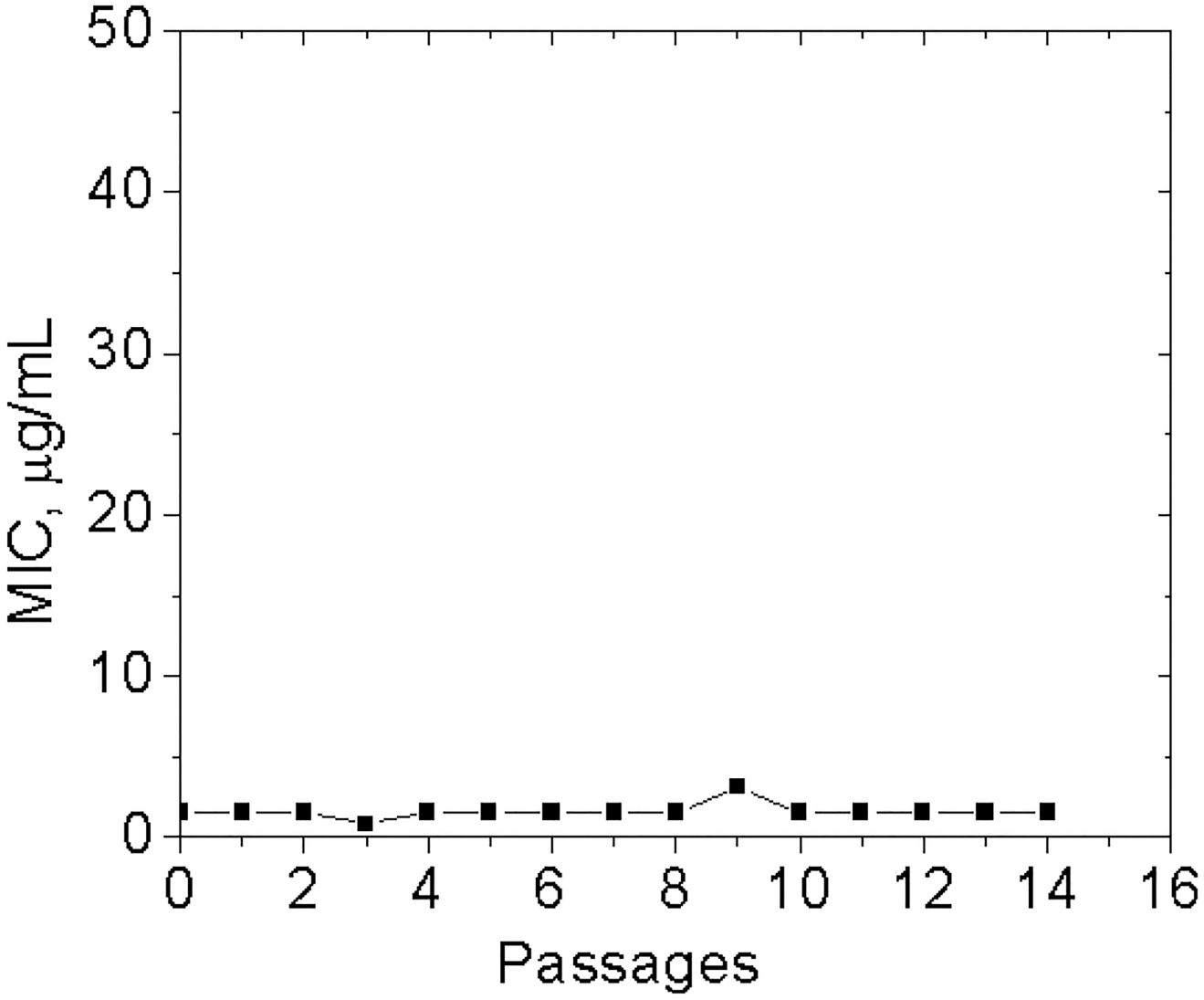

Figure 6.
Drug resistance study for compound **22**.

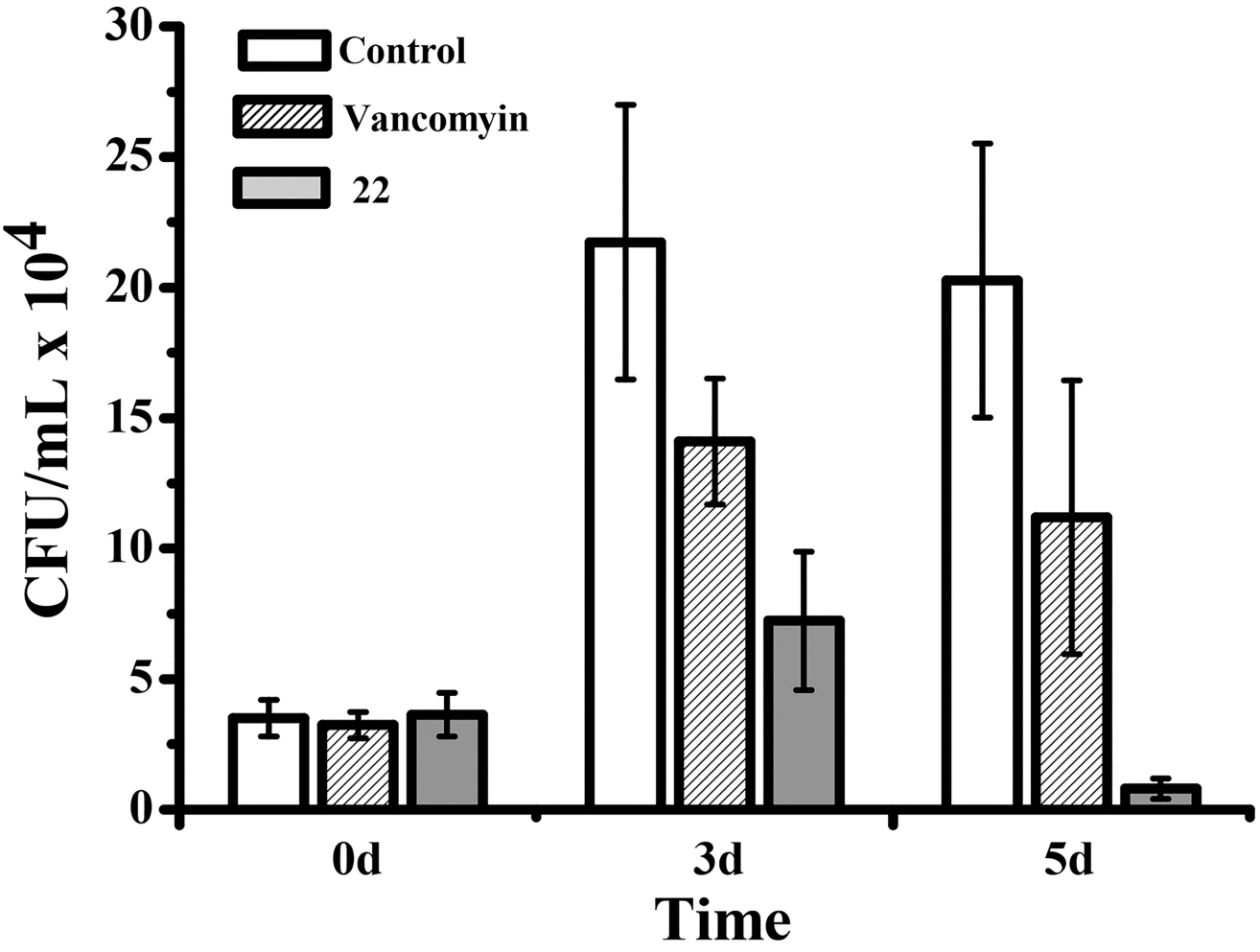

Figure 7.

In vivo efficacy of the compound **22** in a rat model bearing MRSA pneumonia. Rats (n = 6 per group) were inoculated with 100 μL of 10^6 CFU/mL MRSA by intratracheal instillation for 24 h (0 days), followed by intravenous injection of **22** (10 mg/kg) in the tail vein. Bacterial counts were evaluated after 3 and 5 days.

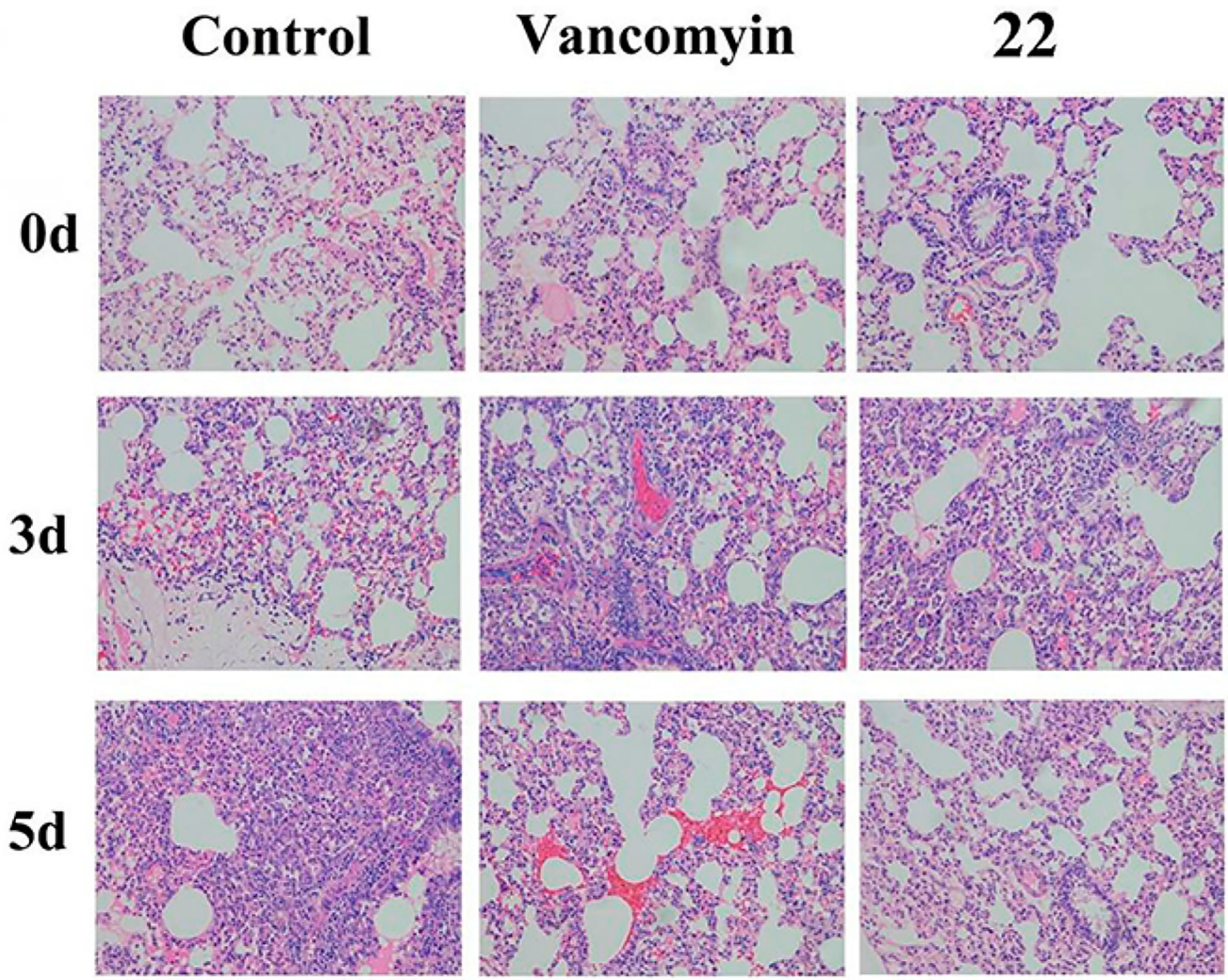

Figure 8.
Pathological assay based on hematoxylin and eosin (H&E) staining.

Table 1

Activity of Lipidated Cationic Hydantoins[a]

Compound	MIC (μg/mL)					
	Gram Positive			Gram Negative		
	MRSA	MRSE	VREF	*E. coli*	*P. A.*	*K. P.*
1	>50	>50	>50	>50	>50	>50
2	>50	>50	>50	12.5	>50	>50
3	6.25	6.25	6.25	3.12	12.5	6.25
4	3.12	3.12	3.12	3.12	>50	12.5
5	>50	>50	>50	>50	>50	>50
6	12.5	25	25	6.25	25	12.5
7	6.25	6.25	6.25	6.25	>50	12.5
8	6.25	6.25	6.25	>50	>50	>50
9	25	>50	>50	12.5	>50	25
10	6.25	6.25	12.5	6.25	12.5	6.25
11	3.12	6.25	6.25	12.5	>50	6.25
12	3.12	25	25	>50	>50	>50
13	6.25	6.25	12.5	6.25	12.5	6.25
14	6.25	6.25	6.25	12.5	>50	>50
15	3.12	3.15	6.25	>50	>50	>50
16	>50	>50	>50	>50	>50	>50
17	>50	>50	>50	>50	>50	>50
18	25	25	25	12.5	12.5	12.5
19	6.25	6.25	6.25	6.25	>50	25
20	3.12	6.25	6.25	>50	>50	>50
21	6.25	6.25	12.5	6.25	6.25	6.25
23	12.5	12.5	12.5	>50	>50	>50
24	12.5	12.5	12.5	>50	>50	>50

Compound	MIC (μg/mL)					
	Gram Positive			Gram Negative		
	MRSA	MRSE	VREF	*E. coli*	*P. A.*	*K. P.*
25	>50	>50	>50	>50	>50	>50

[a]Bacteria included in the test were methicillin-resistant *S. aureus* (MRSA) (ATCC 33591), methicillin-resistant *S. epidermidis* (MRSE) (RP62A), vancomycin-resistant *E. faecalis* (ATCC 700802), *E. coli* (ATCC 25922), *P. aeruginosa* (ATCC 27853), *K. pneumoniae* (ATCC 13383).[44] MIC was measured after incubating hydantoins with bacteria for 16 h. Nitrofurantoin (compound **26**, shown in blue) was included in the test as the positive control. The most potent compound, **22**, is shown in red.

Table 2

Selectivity of Hydantoin Compounds[a]

Compound	MIC of MRSA (μg/mL)	HC_{50} (μg/mL)	SI (HC_{50}/MIC)
3	6.25	90	14.4
6	12.5	80	6.4
10	6.25	100	16
13	6.25	125	20
18	25	200	8
21	6.25	100	16

[a] HC_{50} is the hemolytic activity of the compounds. SI is the selectivity index, which is the ratio of the MIC for MRSA to hemolytic activity. Nitrofurantoin (compound **26**, shown in blue) was included in the test as the positive control. The most potent compound, **22**, is shown in red.